



**HAL**  
open science

# An efficient adaptive strategy to master the global quality of viscoplastic analysis

Jean-Pierre Pelle, David Ryckelynck

► **To cite this version:**

Jean-Pierre Pelle, David Ryckelynck. An efficient adaptive strategy to master the global quality of viscoplastic analysis. *Computers & Structures*, 2000, 78 (1-3), pp.169-183. 10.1016/S0045-7949(00)00107-3 . hal-03760220

**HAL Id: hal-03760220**

**<https://hal.science/hal-03760220>**

Submitted on 2 Mar 2023

**HAL** is a multi-disciplinary open access archive for the deposit and dissemination of scientific research documents, whether they are published or not. The documents may come from teaching and research institutions in France or abroad, or from public or private research centers.

L'archive ouverte pluridisciplinaire **HAL**, est destinée au dépôt et à la diffusion de documents scientifiques de niveau recherche, publiés ou non, émanant des établissements d'enseignement et de recherche français ou étrangers, des laboratoires publics ou privés.



Distributed under a Creative Commons Attribution - NonCommercial 4.0 International License

# An efficient adaptive strategy to master the global quality of viscoplastic analysis

J.-P. Pelle, D. Ryckelynck <sup>\*,1</sup>

L.M.T.  $\pm$  Cachan, ENS de Cachan, CNRS, Université Paris 6, 61, avenue du Président Wilson, 94235 Cachan Cedex, France

To control the numerical quality of non-linear simulations allows to automate the choice of discretisation. Within the framework of time dependent problems, this quality depends on the error made in the calculation of the deformation history. Generally, a kind of expert analysis precedes the satisfying computation. In practice, this analysis could be an optimisation of numerical approximations. We propose a strategy herein, which naturally includes this expert analysis stage. The desired solution is built iteratively, improving all of the history at each iteration, thanks to the LATIN method. A global error estimator is provided by the dissipation error. To pilot the adaptive computation, we propose a partition of this estimator into indicators associated with each kind of error contribution.

*Keywords:* Error estimates; Adaptivity; Non-linear analysis; Latin method; Viscoplasticity

## 1. Introduction

Nowadays, the industry requires the resolution of highly complex problems: 3D problems, non-linear material behaviours, contacts, large deformations, etc. Ahead of solution of such problems, it is necessary to take into account various economical aspects, which are very important: computation time, time necessary to prepare the computation (especially the meshing of complex structures). For a given resolution algorithm, adaptive computation allows us to minimise the computational costs while obtaining a prescribed accuracy by mastering the parameters of the computation (size and type of elements, time increment length). This has been done first in case of linear problems like elasticity [1–3]. And, the proposed methods have been extended to some non-linear time-dependent problems [4–7]. Re-

garding the latter problems, all the adaptive computations proposed are based on the incremental resolution method. Although a non-incremental method, called LATIN method [8,9], allows us to treat problems of non-linear material behaviours, contacts, or large deformations.

As the incremental method is not the only approach to solve non-linear time-dependent problems, we can wonder if it is the most suitable method to build an adaptive strategy characterised by a short computation time and robust error control. In this work, we address this issue by considering the use of the LATIN method to build a non-incremental adaptive strategy. To control conveniently the numerical approximations, we studied the computation of viscoplastic structures with standard constitutive equations [10], on the assumption of small displacements and for quasi-static loading. But numerous other non-linear time-dependant problems could have been studied to build a similar strategy.

The LATIN method is an iterative method to improve approximate solution defined on all the structure and on all the history studied. In the case studied, as well as in Newton's method, the goal of the iterations is to

---

\*Corresponding author.

<sup>1</sup> Now at: ENSAM, LMS-ENSAM, 151, boulevard de l'Hôpital, 75013 Paris, France. Tel: +1-44-24-64-38; fax: +1-44-24-64-68.

treat the non-linearities. But here it is realised on the whole history. A discrete representation of the solution is obviously used. In our approach, this representation is built on a base of space functions computed by employing the finite element method. On this base, the components of an approximate solution are scalar time functions.

To reduce the computational cost, we have proposed an adaptive strategy, in which the improvement of the solution representation is due to the improvement of the treatment of the non-linear equations. A coarse discretisation must be chosen at the beginning of the adaptive strategy. An initial solution is provided through an elastic computation on the interval studied. According to the flaws in the elastic approximation, an error indicator provides a level of non-linearity for the studied problem. In the case of significant non-linearity, LATIN iterations are initiated with the coarse time and space representation, and this representation then becomes more precise over the course of the iterations.

Errors in constitutive equation, especially dissipation error [9], provide a global error estimator, which characterises the distance between an admissible solution and the exact solution. We propose an analytical partition of the global error into indicators associated with each error contributions (time, space, and iteration defaults). Hence, the goal of the main piloting criteria is chosen to obtain a balanced contribution of each kind of error indicator during the computation. The computation is stopped when the global error satisfies the prescribed quality.

The layout of this paper is the following: A brief analysis of existing adaptive strategies enables us to discuss the drawbacks and advantages of the incremental approach. The equations of the viscoplastic reference problem are introduced in Section 2 together with the definition of the dissipation error estimator. A straightforward LATIN algorithm is proposed to solve the reference problem in Section 3. At the end of this section, an example of time and space representation is given. Section 4 outlines some error indicators used for the piloting criteria. And at last, the non-incremental adaptive strategy proposed is described in Section 5, where numerical examples also show the reliability and the efficiency of our approach.

## 2. Adaptive strategy for incremental resolution

By adaptive strategy, we exactly mean the way to organise the numerical resolution, the error control procedure and the parameter adaptation. It could be a mesh adaptation or a time discretisation adaptation for example (Fig. 1). The difficulties encountered to build such strategy are common to numerous time-dependent problems. Hence, we extend our analysis from visco-

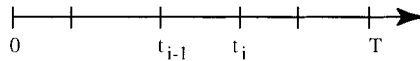


Fig. 1. Time discretisation.

plastic or plastic problems to dynamic problems. Throughout the studied strategy, the resolution method is an incremental one. We will present its principle before dealing with different strategies.

### 2.1. A few remarks about the incremental resolution method

A good modelling of viscoplastic phenomena requires to take into account the history of the deformation. Kinematic constraints and equilibrium equations are similar to those of an elastic problem. To study quasi-static transformation, their definition is merely extended on the time interval  $[0, T]$ . The constitutive equation can be formalised by a non-linear equation linking local stresses to a strain history.

The usual incremental method consists in dividing the time interval  $[0, T]$  into a sequence of subintervals  $[t_{i-1}, t_i]$  associated with time steps.

Generally, on each subinterval the displacement evolution is supposed to be linear:

$$\underline{U}(\underline{M}, t) = \frac{\underline{U}_i(\underline{M}) - \underline{U}_{i-1}(\underline{M})}{t_i - t_{i-1}} (t - t_{i-1}) + \underline{U}_{i-1}(\underline{M}), \quad (1)$$

where  $\underline{M}$  is the current point of the structure.

Consequently, the stresses at the instant  $t_i$  depend on the value of the displacements in  $t_0, t_1, \dots, t_i$  only. The state of the structure being sufficiently known at the instant  $t_{i-1}$ , the problem is to find displacements at the instant  $t_i$ , satisfying kinematic equations and being the solution of time-independent non-linear equations. Such equations are associated to equilibrium equations at the instant  $t_i$  through the constitutive relation. They are solved through a Newton-type iterative method [11]. During the iterations, stresses in equilibrium and stresses satisfying constitutive equations are successively built. Usually the displacement finite element method is associated with the incremental method. Consequently, the equilibrium stresses satisfy the equilibrium equation in a restricted manner only.

### 2.2. The step-by-step strategy

We start with strategies for which the adaptation is done during the resolution. Such strategies consist in improving the discretisation while successively treating the time steps. Generally, during a computation without any adaptation, the errors accumulate as the time increases. The minimum quality to respect is defined by

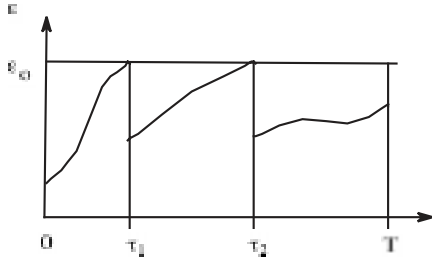


Fig. 2. Adaptation with a maximum relative error.

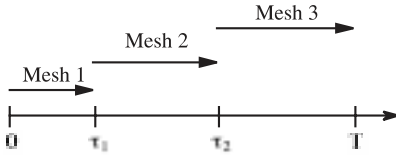


Fig. 3. The step-by-step strategy.

the user who prescribes, according to the kind of criterion used, either:

- the maximum relative error  $\varepsilon_0$  allowed on interval  $[0, t]$  for each instant  $t$  of  $[0, T]$  (the part of error, which is independent of the deformation history can be modified by an adaptation of the mesh) [5] (Fig. 2);
- or a maximum value for error contribution of each time step [12–15].

During the computation, the time interval is subdivided into adaptive periods with quality criteria. The transition between the two periods is associated to an adaptation (Fig. 3). After an adaptation, the computation is usually repeated again on the last time step of the adaptive period, in order to improve the quality before continuing the computation.

This kind of strategy is used to adapt the mesh in Refs. [13,14] for dynamic analyses and in Refs. [5,12] for plastic and viscoplastic analyses. Obviously, to continue the computation with the adapted mesh, some initial data, at the beginning of the step, are transferred from the old mesh. Time adaptation is proposed with this strategy in Ref. [16] for viscoplastic analyses while time and space discretisation are together adapted in Ref. [17] for dynamic analyses and in Ref. [15] for plastic analyses.

In non-linear cases when, due to mesh adaptation, the computation is performed again on a step, a rather good solution defined on the previous mesh is known. In Ref. [18], the authors propose reducing the cost of the non-linear treatment by using this solution to initialise the iterative resolution on the step. This is performed with a hierarchical mesh adaptation associated with a sort of multigrid resolution of equilibrium equations.

One of the main advantages of an adaptation during the resolution is to take into account the mechanical information obtained through the previous computa-

tion, thanks to a transfer of initial data, or moreover, thanks to the last approach presented above.

### 2.3. The multi-resolution stage strategy

All of the deformation history contributes to the error at instant  $t$ . If the adaptation periods are too long, the error induced during the former instant can be dominant and may not be reduced by an adaptation in the following instant. In this case, it is more suitable to use a strategy, which allows improving the description of all the deformation history. But, because of the incremental resolution method, this becomes possible only with a new resolution started at the beginning.

This kind of strategy is used at the LMT for plastic or viscoplastic analyses with several stages of resolution [5,19,20]. In practice, in these works, the same mesh is used on all the time interval. A first mesh is obtained through an adaptive elastic computation for the maximum loading. Then, after each resolution with error control, the mesh and eventually some other parameters are adapted to optimise the computation of a solution with the required quality (Fig. 4).

In the cases of simple problems, only two stages are needed. A time varying mesh has been used with this strategy to improve the optimality for dynamic analyses [13,21]. The problem is completely solved with an initial coarse mesh. During the coarse mesh run, assessments are made at selected intervals, from which the level of adaptation for each adaptation interval is selected. This time varying mesh is then used to make a second complete run (Fig. 5).

We can note that mesh adaptation is not always sufficient to master the quality of plastic or viscoplastic analyses. In fact, the time discretisation and the accuracy of the iterative Newton algorithm must usually be

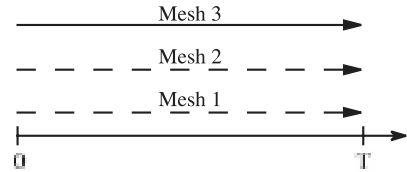


Fig. 4. The multi-resolution stage strategy.

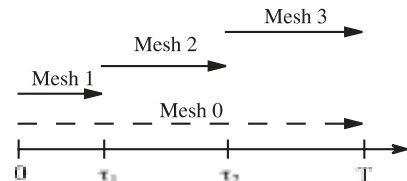


Fig. 5. Time varying mesh.

adapted. Such adaptations have been proposed in Refs. [19,20].

#### 2.4. Advantages and drawbacks

Both the strategies presented above have their own drawbacks and advantages: On the one hand, the multi-resolution stage strategy allows a robust error control. But its costs can be worrisome in case of non-linear analyses, because the intermediate solutions are used only for their defaults although they provide mechanical pieces of information. On the other hand, the step-by-step strategy takes into account the previous computation, with only small returns (in few steps). But it can't allow a robust error control, because the error is estimated a posteriori. It is therefore known only when the computation is finished. The incremental resolution method does not seem, then, to be appropriate to build an adaptive strategy with a robust error control and efficient simulation.

In the strategy proposed here, approximate solutions can be improved over all the time interval through an iterative approach: the LATIN method. As the approximate solution is defined on all the time interval, the global error can be checked at the end of each iteration. And thanks to the iterative approach, the previous computation is obviously taken into account.

### 3. Properties of the equations to be solved

#### 3.1. The reference problem

We suppose that the structure is a domain  $\Omega$ . On a part  $\partial_1\Omega$  of the boundary  $\partial\Omega$ , we suppose that the imposed displacement field is  $\underline{U}_d$  (Fig. 6). On the complementary part  $\partial_2\Omega$ , density of forces  $\underline{F}_d$  is imposed. Moreover,  $\Omega$  is submitted to a density of body forces  $\underline{f}_d$ .

In viscoplasticity, the value of the stress at  $\mathbf{t}$  is a function of the history of the strain at the instant  $\mathbf{t}$ , and this function may be expressed at each current point  $\underline{M}$  of the structure  $\Omega$ , by the relation:

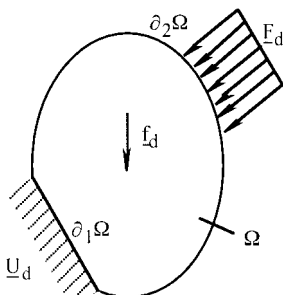


Fig. 6. The loading.

$$\boldsymbol{\sigma}_t = \mathbf{A}(\boldsymbol{\varepsilon}_{|t}, \tau \leq t), \quad (2)$$

where  $\mathbf{A}$  is an operator characteristic of the material and  $\boldsymbol{\varepsilon}$  is the strain field. In case of stable constitutive equation, the knowledge of such a relationship between stresses and strains is sufficient to give a solution which respects kinematic equations and equilibrium equations. To make everything simple, a common way to describe this relationship is to use internal variables in the framework of thermodynamics. It has been shown that different choices of internal variables can make it possible to formulate a given relationship between stresses and strains [9]. A convenient formulation for computation is a normal formulation in which equations of state are linear [9]. This formulation is obtained from the classical one by changing a set of internal variables. Moreover we suppose that the model is standard [10]. This means that evolution laws are obtained from a viscoplastic potential.

The internal variables are the plastic strain  $\boldsymbol{\varepsilon}^p$ , a tensor  $\boldsymbol{\alpha}$  associated with the kinematic hardening  $\boldsymbol{\beta}$  and a scalar  $p$  associated to the isotropic hardening  $R$ . We use the simplified notations  $\mathbf{X} = (\boldsymbol{\alpha}, p)$ ,  $\mathbf{Y} = (\boldsymbol{\beta}, R)$ . Therefore, the problem to be solved can be described as follows.

Reference problem  $P_{\text{ref}}$ : to find the dissipation quantities  $s = (\dot{\boldsymbol{\varepsilon}}^p, \dot{\mathbf{X}}, \boldsymbol{\sigma}, \mathbf{Y})$  such that

$$\text{kinematic equation: } \underline{U} \in \mathcal{U}_{\text{ad}}^{[0,T]}$$

$$\forall t \in [0, T], \quad \underline{U}|_{\partial_1\Omega} = \underline{U}_d, \quad (3)$$

$$\text{equilibrium equation: } \boldsymbol{\sigma} \in \mathcal{S}_{\text{ad}}^{[0,T]}$$

$$\forall t \in [0, T] \quad \forall \underline{U}^* \in \mathcal{U}_0, \quad (4)$$

$$- \int_{\Omega} \text{Tr}[\boldsymbol{\sigma} \boldsymbol{\varepsilon}(\underline{U}^*)] d\Omega + \int_{\Omega} \underline{f}_d \cdot \underline{U}^* d\Omega + \int_{\partial_2\Omega} \underline{F}_d \cdot \underline{U}^* dS = 0,$$

constitutive relations:  $\forall \underline{M} \in \Omega$ ,  
initial state

$$\boldsymbol{\sigma}_{t=0} = 0, \quad \mathbf{Y}_{t=0} = 0, \quad (5)$$

equations of state

$$\boldsymbol{\varepsilon}^e = \mathbf{K}^{-1} \boldsymbol{\sigma}, \quad \mathbf{X} = \mathbf{A}\mathbf{Y} \quad \forall t \in [0, T], \quad (6)$$

evolution laws

$$\dot{\boldsymbol{\varepsilon}}^p = \partial_{\boldsymbol{\sigma}} \varphi^*, \quad -\dot{\mathbf{X}} = \partial_{\mathbf{Y}} \varphi^* \quad \forall t \in [0, T], \quad (7)$$

where  $\mathcal{U}_0$  is defined by

$$\mathcal{U}_0 = \{ \underline{U}(\underline{M}) \underline{M} \in \Omega \mid \underline{U}|_{\partial_1\Omega} = 0 \}. \quad (8)$$

We are also going to use  $\mathcal{S}_0$  defined by

$$\mathcal{S}_0 = \left\{ \boldsymbol{\sigma}(\underline{M}) \underline{M} \in \Omega \mid \int_{\Omega} \text{Tr}[\boldsymbol{\sigma} \boldsymbol{\varepsilon}(\underline{U}^*)] d\Omega = 0 \quad \forall \underline{U}^* \in \mathcal{U}_0 \right\}. \quad (9)$$

The material behaviour is characterised by

$$\varphi^*(\boldsymbol{\sigma}, \mathbf{Y}) = \frac{k}{m+1} \langle z \rangle_+^{m+1}, \quad (10)$$

$$z = \|\boldsymbol{\sigma}^D - \boldsymbol{\beta}\| + \frac{1}{2} \frac{a}{c} \|\boldsymbol{\beta}\|^2 - 1(R) - R_0, \quad (11)$$

$$\|\bullet\|^2 = \text{Tr}[(\bullet)^2], \quad (12)$$

$$1(R) = \mathcal{Q} \frac{R}{R_s} \left( 2 - \frac{R}{R_s} \right) \quad \text{for } R \leq R_s, \quad (13)$$

where  $\boldsymbol{\sigma}^D$  is the deviatoric part of  $\boldsymbol{\sigma}$ , and  $\mathbf{K}$  and  $\mathcal{A}$  are characteristic operators.

The reference problem is a global non-linear one. But some of the equations are linear and others are local. In fact non-linear equations, evolution equations, are local. In order to use this feature, we say that  $s = (\dot{\boldsymbol{\varepsilon}}^P, \dot{\mathbf{X}}, \boldsymbol{\sigma}, \mathbf{Y})$  is *admissible* if and only if it satisfies all the linear equations, i.e. all except evolution laws. We then write  $s \in A_d$ . If  $(\dot{\boldsymbol{\varepsilon}}^P, \dot{\mathbf{X}}, \boldsymbol{\sigma}, \mathbf{Y})$  confirms the non-linear evolution laws, we write:  $s \in \Gamma$ . So, the exact solution of the reference problem  $s_{\text{ex}}$  must satisfy:  $s_{\text{ex}} = \Gamma \cap A_d$ .

### 3.2. The dissipation error estimator

The constitutive formulation being a normal and standard one, an error in constitutive equation allows to value the way non-linear equations are solved. This error is based on Legendre–Fenchel inequality:

$$\begin{aligned} \forall (\dot{\boldsymbol{\varepsilon}}^P, \dot{\mathbf{X}}, \boldsymbol{\sigma}, \mathbf{Y}) \quad & \varphi(\dot{\boldsymbol{\varepsilon}}^P, -\dot{\mathbf{X}}) + \varphi^*(\boldsymbol{\sigma}, \mathbf{Y}) - \text{Tr}[\boldsymbol{\sigma} \dot{\boldsymbol{\varepsilon}}^P] \\ & + \mathbf{Y} \circ \dot{\mathbf{X}} \geq 0, \end{aligned} \quad (14)$$

where  $\text{Tr}[\boldsymbol{\sigma} \dot{\boldsymbol{\varepsilon}}^P] - \mathbf{Y} \circ \dot{\mathbf{X}}$  is the dissipation and  $\varphi$  is the dual function of  $\varphi^*$ :

$$\varphi(\dot{\boldsymbol{\varepsilon}}^P, -\dot{\mathbf{X}}) = \text{Sup}_{(\boldsymbol{\sigma}, \mathbf{Y})} \{ \text{Tr}[\boldsymbol{\sigma} \dot{\boldsymbol{\varepsilon}}^P] - \mathbf{Y} \circ \dot{\mathbf{X}} - \varphi^*(\boldsymbol{\sigma}, \mathbf{Y}) \}. \quad (15)$$

A global distance in evolution laws can be defined:

$$s \in \Gamma \iff e(s) = 0 \quad (16)$$

with

$$\begin{aligned} e(s) = \int_0^T \int_{\Omega} \{ & \varphi(\dot{\boldsymbol{\varepsilon}}^P, -\dot{\mathbf{X}}) + \varphi^*(\boldsymbol{\sigma}, \mathbf{Y}) - \text{Tr}[\boldsymbol{\sigma} \dot{\boldsymbol{\varepsilon}}^P] \\ & + \mathbf{Y} \circ \dot{\mathbf{X}} \} d\Omega dt. \end{aligned} \quad (17)$$

We therefore obtain a dissipation error estimator [9] associated to the reference problem  $P_{\text{ref}}: e_{\text{ref}} = e(s)$  with  $s \in A_d$ , to quantify the quality of  $s \in A_d$  in terms of approximation of  $s_{\text{ex}}$ .

A relative error estimator is obtained by Ref. [20]:

$$\varepsilon_{\text{ref}} = \frac{e_{\text{ref}}}{D} \quad (18)$$

with  $D = 4 \text{Sup}_{t \in [0, T]} d_t$  and

$$\begin{aligned} d_t &= \frac{1}{2} \text{diss}_t + \frac{1}{2} \text{ener}_t \text{diss}_t \\ &= \int_0^t \int_{\Omega} \text{Max}(\varphi(\dot{\boldsymbol{\varepsilon}}^P, \dot{\mathbf{X}}) \\ &\quad + \varphi^*(\boldsymbol{\sigma}, \mathbf{Y}), \frac{R_0 \text{Tr}[\mathbf{K}^{-1} \boldsymbol{\sigma} \dot{\boldsymbol{\varepsilon}}^P]}{\|\boldsymbol{\sigma}^D\|}) d\Omega d\tau, \\ \text{ener}_t &= \frac{1}{2} \int_{\Omega} \text{Tr}[\mathbf{K}^{-1} \boldsymbol{\sigma} \boldsymbol{\sigma}] + \mathcal{A}^{-1} \mathbf{Y} \cdot \mathbf{Y} d\Omega \end{aligned}$$

with the property:  $s \in A_d$  and  $e(s) = 0$  if and only if  $s = s_{\text{ex}}$ .

$e(s)$  with  $s \in A_d$  is then a global error estimator, which takes account of all the defaults that contribute to the exact error:  $s - s_{\text{ex}}$ .

## 4. A non-incremental resolution

In this section, we present the numerical algorithm that is used to approximately solve the reference problem. It is built in the framework of the LATIN method introduced by Ladevèze in 1985 [8,9]. In the first part of this section, we present a base-line algorithm common to other implementations of the method. This algorithm is completely defined without any discretisation. Then, we describe the way we use a discretisation to build an efficient and robust algorithm. An example is presented to explain the base of space functions used to obtain a numerical representation of the solution on all of the time interval and on all of the domain  $\Omega$ .

### 4.1. The LATIN method

The LATIN method contrasts with the incremental method in the sense that it is not built on the time step notion. It is not necessary to subdivide  $[0, T]$  into increments to define a LATIN algorithm. The three basic principles of the method are

*P1:* In order to separate the difficulties, we create two groups of equations

- a group of local equations, eventually non-linear,
- a group of linear equations, eventually global.

*P2:* The approach is an iterative one, which provides a solution of each group of equations at each iteration (Fig. 7).

*P3:* An appropriate representation defined on  $\Omega \times [0, T]$  has to be used to solve the global equations.

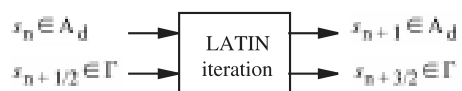


Fig. 7. The LATIN iteration.

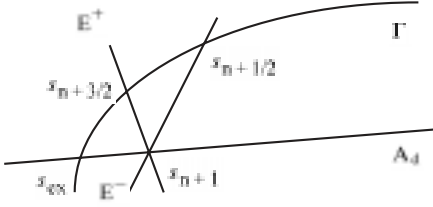


Fig. 8. Search directions.

The search for a solution for the first group of equation is called local stage and the global stage is the search for a solution for the second group. Search directions are defined to solve one stage after the other, in order to obtain a unique solution of good quality (Fig. 8).

The LATIN initialisation can be done through an elastic computation on all the time interval, followed by a local stage. The elastic computation consists in searching for  $s_0 \in A_d \cap \Gamma_e$  with

$$\Gamma_e = \{(\dot{\epsilon}^p, \dot{\mathbf{X}}, \boldsymbol{\sigma}, \mathbf{Y}) \mid (\dot{\epsilon}^p, \dot{\mathbf{X}}) = (0, 0) \forall t \in [0, T] \forall \underline{M} \in \Omega\}. \quad (19)$$

Thanks to the normal formulation of the constitutive equations, we can use the real subspace tangent to  $\Gamma$  (characterised by the operator  $\mathbf{H}$ ) to define  $E^-$ :

$$E^- = \left\{ (\Delta \dot{\epsilon}^p, \Delta \dot{\mathbf{X}}, \Delta \boldsymbol{\sigma}, \Delta \mathbf{Y}) \mid \begin{bmatrix} \Delta \dot{\epsilon}^p \\ -\Delta \dot{\mathbf{X}} \end{bmatrix} = \mathbf{H} \begin{bmatrix} \Delta \boldsymbol{\sigma} \\ \Delta \mathbf{Y} \end{bmatrix} \forall t \in [0, T] \forall \underline{M} \in \Omega \right\}. \quad (20)$$

For  $E^+$ , we choose a very simple approach:

$$E^+ = \{(\Delta \dot{\epsilon}^p, \Delta \dot{\mathbf{X}}, \Delta \boldsymbol{\sigma}, \Delta \mathbf{Y}) \mid (\Delta \boldsymbol{\sigma}, \Delta \mathbf{Y}) = (0, 0) \forall t \in [0, T] \forall \underline{M} \in \Omega\}. \quad (21)$$

At the iteration  $n+1$ ,  $s_n$  and  $s_{n+1/2}$  are known and the two stages are as follows:

*Global stage:* to find  $s_{n+1} \in A_d$  such that

$$\forall t \in [0, T] \quad \forall \underline{M} \in \Omega, \quad (22)$$

$$\begin{bmatrix} \dot{\epsilon}_{n+1}^p \\ -\dot{\mathbf{X}}_{n+1} \end{bmatrix} = \begin{bmatrix} \dot{\epsilon}_{n+1/2}^p \\ -\dot{\mathbf{X}}_{n+1/2} \end{bmatrix} + \mathbf{H} \begin{bmatrix} \boldsymbol{\sigma}_{n+1} - \boldsymbol{\sigma}_{n+1/2} \\ \mathbf{Y}_{n+1} - \mathbf{Y}_{n+1/2} \end{bmatrix}.$$

*Local stage:* to find  $s_{n+3/2} \in \Gamma$ , such that

$$\forall t \in [0, T] \quad \forall \underline{M} \in \Omega \quad \begin{cases} \boldsymbol{\sigma}_{n+3/2} = \boldsymbol{\sigma}_{n+1}, \\ \mathbf{Y}_{n+3/2} = \mathbf{Y}_{n+1}. \end{cases} \quad (23)$$

Numerous choices of search directions can be used, with reserve that the local stage is still local and that the global stage is still linear. For materials which verify Drucker's inequality, the conditions about  $E^+$  and  $E^-$  which ensure the convergence of the method are developed in Ref. [9]. But this approach cannot be used easily.

This is why we chose above, the search directions used in Ref. [22] for viscoplastic analysis.

In practice, the local stage is very easy to solve because the solution is explicit. It is not the same for the global stage, which is the most costly stage of the algorithm. This is why the third principle *P3* is introduced to use a suitable approximate resolution of this stage. In order to do so, a variational formulation is required [9]. Admissible thermodynamic forces are searched firstly and then other admissible variables are computed.

The previous admissible thermodynamic forces are known. So, we can search for their correction. The formulation is based on the strain compatibility equation.

*Global stage*

(1) to find  $(\boldsymbol{\sigma}_{n+1}, \mathbf{Y}_{n+1})(\underline{M}, t) \Omega \times [0, T]$  such that

$$(\boldsymbol{\sigma}_{n+1}, \mathbf{Y}_{n+1}) = (\boldsymbol{\sigma}_n, \mathbf{Y}_n) + (\Delta \boldsymbol{\sigma}_{n+1}, \Delta \mathbf{Y}_{n+1}), \quad (24)$$

$$\forall \underline{M} \in \Omega \quad (\Delta \boldsymbol{\sigma}_{n+1}, \Delta \mathbf{Y}_{n+1})|_{t=0} = 0, \quad (25)$$

$$\forall t \in [0, T] \quad \Delta \boldsymbol{\sigma}_{n+1}|_t \in \mathcal{S}_0, \quad (26)$$

$$\begin{aligned} & \int_0^T \int_{\Omega} \{ \text{Tr}[\mathbf{K}^{-1} \Delta \dot{\boldsymbol{\sigma}}_{n+1} \boldsymbol{\sigma}^*] + \Lambda^{-1} \Delta \dot{\mathbf{Y}}_{n+1} \cdot \mathbf{Y}^* \} d\Omega dt \\ & + \int_0^T \int_{\Omega} \mathbf{H} \begin{bmatrix} \Delta \boldsymbol{\sigma}_{n+1} \\ \Delta \mathbf{Y}_{n+1} \end{bmatrix} \cdot \begin{bmatrix} \boldsymbol{\sigma}^* \\ \mathbf{Y}^* \end{bmatrix} d\Omega dt \\ & = \int_0^T \int_{\Omega} \begin{bmatrix} \dot{\epsilon}_n^p - \dot{\epsilon}_{n+1/2}^p \\ -(\dot{\mathbf{X}}_n - \dot{\mathbf{X}}_{n+1/2}) \end{bmatrix} \cdot \begin{bmatrix} \boldsymbol{\sigma}^* \\ \mathbf{Y}^* \end{bmatrix} d\Omega dt \end{aligned} \quad (27)$$

$\forall (\boldsymbol{\sigma}^*, \mathbf{Y}^*)$  with  $\boldsymbol{\sigma}_t^* \in \mathcal{S}_0 \forall t \in [0, T]$  and

$$(\boldsymbol{\sigma}^*, \mathbf{Y}^*)|_{t=0} = 0 \quad \forall \underline{M} \in \Omega.$$

(2) to find the displacement  $\underline{U}_{n+1} \in \mathcal{W}_{ad}^{[0, T]}$ , such that (search direction is satisfied):

$$\|\boldsymbol{\epsilon}(\underline{U}_{n+1}) - \dot{\boldsymbol{\epsilon}}\|_{\mathbf{K}, \Omega \times [0, T]} \sim \underset{\underline{V} \in \mathcal{W}_{ad}^{[0, T]}}{\text{Min}} \|\boldsymbol{\epsilon}(\dot{V}) - \dot{\boldsymbol{\epsilon}}\|_{\mathbf{K}, \Omega \times [0, T]} \quad (28)$$

with

$$\begin{aligned} \dot{\boldsymbol{\epsilon}} & \sim \mathbf{K}^{-1} \dot{\boldsymbol{\sigma}}_{n+1} + \dot{\epsilon}_{n+1/2}^p + \mathbf{H}_{\sigma\sigma}(\boldsymbol{\sigma}_{n+1} - \boldsymbol{\sigma}_{n+1/2}) \\ & + \mathbf{H}_{\sigma\mathbf{Y}}(\mathbf{Y}_{n+1} - \mathbf{Y}_{n+1/2}) \text{ and } \|\boldsymbol{\epsilon}\|_{\mathbf{K}, \Omega \times [0, T]}^2 \\ & = \int_0^T \int_{\Omega} \text{Tr}[\mathbf{K} \boldsymbol{\epsilon} \boldsymbol{\epsilon}] d\Omega dt. \end{aligned}$$

When no space approximation is used to search for the admissible forces, the solution of this problem of minimisation is such that:

$$\boldsymbol{\epsilon}(\underline{U}_{n+1}) = \dot{\boldsymbol{\epsilon}} \quad \forall t \in [0, T] \quad \forall \underline{M} \in \Omega. \quad (29)$$

(3) the other quantities are computed through the equations of state (6):

$$\forall t \in [0, T] \quad \forall \underline{M} \in \Omega \begin{cases} \dot{\mathbf{x}}_{n+1}^p = \boldsymbol{\varepsilon}(\dot{\underline{U}}_{n+1}) - \mathbf{K}^{-1} \dot{\boldsymbol{\sigma}}_{n+1}, \\ \dot{\mathbf{X}}_{n+1} = A \dot{\mathbf{Y}}_{n+1}. \end{cases} \quad (30)$$

All the variables can be deduced from the admissible thermodynamic forces and the displacement. The numerical representation must be applied to these quantities.

#### 4.2. The numerical algorithm

In this work, we propose a straightforward representation of the admissible thermodynamic forces. Notice that simple choices can be made in so far as the computations are to be submitted to an error control in all the cases. This representation must allow a simple approximate resolution of the global stage without altering the reliability of the algorithm. For the numerical aspect, scalar time function and classical finite element space function are used.

##### 4.2.1. The representation of admissible thermodynamic forces

We propose to use a base of space functions and a particular solution to represent the admissible forces. This base is entirely built during the LATIN iteration by introducing new space functions before solving the global stage (Fig. 9).

Let suppose that we know

- a set of independent displacement fields defined on  $\Omega$ ,  $(\underline{A}_k)_{k=1, \dots, \text{Nu}}$  such that

$$\underline{A}_k \in \mathcal{U}_0 \quad \forall k \in \{1, \dots, \text{Nu}\}, \quad (31)$$

- a set of independent stress fields defined on  $\Omega$ ,  $(\mathbf{B}_k)_{k=1, \dots, \text{Ns}}$  such that

$$\mathbf{B}_k \in \mathcal{S}_0 \quad \forall k \in \{1, \dots, \text{Ns}\}, \quad (32)$$

- a set of independent fields of complementary thermodynamic force defined on  $\Omega$ ,  $(\mathbf{C}_k)_{k=1, \dots, \text{Ny}}$ .

Moreover, at the iteration number  $n+1$ , the quantities  $(\boldsymbol{\sigma}_n, \mathbf{Y}_n)$  and  $\underline{U}_n$  are known and they respect the following admissible constraints:

$$\boldsymbol{\sigma}_n \in \mathcal{S}_{\text{ad}}^{[0, T]}, \quad (\boldsymbol{\sigma}_n, \mathbf{Y}_n)|_{t=0} = 0 \quad \forall \underline{M} \in \Omega, \quad \underline{U}_n \in \mathcal{U}_{\text{ad}}^{[0, T]}.$$

Thermodynamic forces are searched such that

$$\underline{U}_{n+1}(\underline{M}, t) = \underline{U}_n(\underline{M}, t) + \sum_{k=1}^{\text{Nu}} \alpha_k^{n+1}(t) \underline{A}_k(\underline{M}), \quad (33)$$

$$\boldsymbol{\sigma}_{n+1}(\underline{M}, t) = \boldsymbol{\sigma}_n(\underline{M}, t) + \sum_{k=1}^{\text{Ns}} \beta_k^{n+1}(t) \mathbf{B}_k(\underline{M}), \quad (34)$$

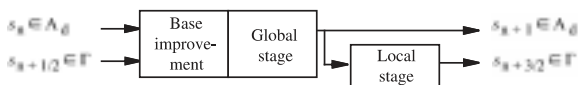


Fig. 9. The approximate resolution of the global stage.

$$\mathbf{Y}_{n+1}(\underline{M}, t) = \mathbf{Y}_n(\underline{M}, t) + \sum_{k=1}^{\text{Ny}} \gamma_k^{n+1}(t) \mathbf{C}_k(\underline{M}), \quad (35)$$

where  $\alpha_k^{n+1}$ ,  $\beta_k^{n+1}$  and  $\gamma_k^{n+1}$  are scalar time functions. In practice, the order of magnitude of Nu, Ns, Ny and  $n$  are quite the same.

Therefore, on the global stage, the unknown factors are the set of time functions:

$$\mathbf{g}^T = [\beta_1^{n+1}, \dots, \beta_{\text{Ns}}^{n+1}, \gamma_1^{n+1}, \dots, \gamma_{\text{Ny}}^{n+1}], \\ \mathbf{a}^T = [\alpha_1^{n+1}, \dots, \alpha_{\text{Nu}}^{n+1}].$$

Two time-dependent differential systems have to be solved:

- (1) to find  $g(t)$  defined on  $[0, T]$  such that

$$\begin{cases} g(0) = 0, \\ \mathbf{G} \dot{g} + \mathbf{M}_t g = \mathbf{Q}_t \quad \forall t \in [0, T], \end{cases} \quad (36)$$

- (2) to find  $a(t)$  defined on  $[0, T]$  such that

$$\begin{cases} a(0) = 0, \\ \mathbf{G} \dot{a} = \mathbf{Q}_t \quad \forall t \in [0, T]. \end{cases} \quad (37)$$

The first differential problem is obtained through Eq. (27) and the second one is obtained through the displacement problem (28).

##### 4.2.2. The improvement of the base of space functions

To improve the base, we firstly generate space functions with the residue of the global stage. Then, if the new function is independent from the previous ones, we keep it to improve the base. Otherwise the base is not improved.

To generate space functions, we search a potential correction for thermodynamic forces  $\Delta \boldsymbol{\sigma}(\underline{M}, t)$  and  $\Delta \mathbf{Y}(\underline{M}, t)$  defined on  $\Omega \times [0, T]$  such that

$$\begin{aligned} \Delta \boldsymbol{\sigma}(\underline{M}, t) &= \delta(t) \mathbf{B}(\underline{M}) \quad \text{with } \mathbf{B} \in \mathcal{S}_0, \\ \Delta \mathbf{Y}(\underline{M}, t) &= \delta(t) \mathbf{C}(\underline{M}), \end{aligned} \quad (38)$$

where  $\delta$  is a known time function built on the distance between  $s_{n+1/2}$  and  $s_n$ .

With the variational formulation (27), we obtain this equation:

$$a_H((\mathbf{B}, \mathbf{C}), (\mathbf{B}^*, \mathbf{C}^*)) = b((\mathbf{B}^*, \mathbf{C}^*)) \quad \forall \mathbf{B}^* \in \mathcal{S}_0 \quad \forall \mathbf{C}^*, \quad (39)$$

where  $b$  is a kind of global stage residue:

$$\begin{aligned} b((\mathbf{B}^*, \mathbf{C}^*)) &= \int_0^T \int_{\Omega} \delta \text{Tr}[(\dot{\boldsymbol{\varepsilon}}_n^p - \dot{\boldsymbol{\varepsilon}}_{n+1/2}^p) \mathbf{B}^*] d\Omega dt \\ &\quad - \int_0^T \int_{\Omega} \delta (\dot{\mathbf{X}}_n - \dot{\mathbf{X}}_{n+1/2}) \cdot \mathbf{C}^* d\Omega dt, \end{aligned}$$

$$\begin{aligned} a_H((\mathbf{B}, \mathbf{C}), (\mathbf{B}^*, \mathbf{C}^*)) &= \frac{1}{2} \delta^2(T) a_K((\mathbf{B}, \mathbf{C}), (\mathbf{B}^*, \mathbf{C}^*)) \\ &\quad + \int_0^T \int_{\Omega} \delta^2 \mathbf{H} \begin{bmatrix} \mathbf{B} \\ \mathbf{C} \end{bmatrix} \cdot \begin{bmatrix} \mathbf{B}^* \\ \mathbf{C}^* \end{bmatrix} d\Omega dt, \end{aligned}$$

where

$$a_K((\mathbf{B}, \mathbf{C}), (\mathbf{B}^*, \mathbf{C}^*)) = \int_{\Omega} \{\text{Tr}[\mathbf{K}^{-1} \mathbf{B} \mathbf{B}^*] \mathbf{A}^{-1} \mathbf{C} \cdot \mathbf{C}^*\} d\Omega.$$

In order to simplify the space function generation, we prefer to treat the following problem: To find  $\mathbf{B} \in \mathcal{S}_0$  and  $\mathbf{C}$  such that

$$a_K((\mathbf{B}, \mathbf{C}), (\mathbf{B}^*, \mathbf{C}^*)) = b((\mathbf{B}^*, \mathbf{C}^*)) \quad \forall \mathbf{B}^* \in \mathcal{S}_0 \quad \forall \mathbf{C}^*. \quad (40)$$

We then obtain a global problem as far as stresses are concerned: To find  $\mathbf{B} \in \mathcal{S}_0$  such that

$$\int_{\Omega} \text{Tr}[(\mathbf{K}^{-1} \mathbf{B} - \boldsymbol{\varepsilon}_b) \mathbf{B}^*] d\Omega = 0 \quad \forall \mathbf{B}^* \in \mathcal{S}_0 \quad (41)$$

$$\text{with } \boldsymbol{\varepsilon}_b = \int_0^T \delta(\dot{\boldsymbol{\varepsilon}}_n^p - \dot{\boldsymbol{\varepsilon}}_{n+1/2}^p) dt$$

and an explicit solution for the other thermodynamic forces:

$$\mathbf{C}(\underline{M}) = -\mathbf{A} \int_0^T \delta(\dot{\mathbf{X}}_n - \dot{\mathbf{X}}_{n+1/2}) dt. \quad (42)$$

Problem (41) is an elastic problem in which a unique displacement field  $\underline{A} \in \mathcal{U}_0$  exists such that

$$\boldsymbol{\varepsilon}(\underline{A}) = \mathbf{K}^{-1} \mathbf{B} - \boldsymbol{\varepsilon}_b. \quad (43)$$

The stress problem (41) is therefore equivalent to the following displacement problem: To find  $\underline{A} \in \mathcal{U}_0$  such that

$$\int_{\Omega} \text{Tr}[(\mathbf{K} \boldsymbol{\varepsilon}(\underline{A}) + \boldsymbol{\varepsilon}_b) \boldsymbol{\varepsilon}(\underline{U}^*)] d\Omega = 0 \quad \forall \underline{U}^* \in \mathcal{U}_0 \quad (44)$$

and  $\mathbf{B} = \mathbf{K} \boldsymbol{\varepsilon}(\underline{A}) + \boldsymbol{\varepsilon}_b \quad \forall \underline{M} \in \Omega$ . This formulation allows us to use the classical displacement approach of the finite element method.

The independence criteria of the space functions are not developed here. The matrix  $\mathbf{G}$  and  $\mathbf{G}$  are in fact matrix of coupling terms between space functions. If and only if those matrix are regular, there is a unique solution of the time problems. We then use this property to propose independence criteria [23].

#### 4.2.3. Numerical approximation

The algorithm presented above is based on continuous problems. These problems are solved through classical numerical approaches.

The space functions are represented through the finite element method. Thus, the displacement field is represented with a matrix of shape functions  $\mathbf{N}$  and a vector of nodal displacement  $q$ :  $\underline{A}_k = \mathbf{N} q_k \forall k \in \{1, \dots, \text{Nu}\}$ .

The space integrals are approached through a Gauss method:

$$\int_{\Omega} f(\underline{M}) d\Omega \rightarrow \sum_i^{\text{Nh}} f(\underline{M}_i) w_i$$

in which  $(\underline{M}_i)_{i=1, \dots, \text{Nh}}$  are the integration points. The quantities  $s_n$  and  $s_{n+1/2}$  except the displacements, have to be defined in space at the integration point.

To represent the time functions we use a partition of the time interval:

$$t_1 = 0 < \dots < t_{i-1} < t_i < \dots < t_{\text{Nt}} = T.$$

The time evolution of the displacements and of the admissible thermodynamic forces are assumed to be linear on  $[t_{i-1}, t_i]$  (Fig. 10).

The time integrals are approached through a  $\theta$ -method built on integration instants  $\tau_{i-1}$  such that

$$\tau_{i-1} = (1 - \theta)t_{i-1} + \theta t_i \quad \text{with } \theta = 0.5.$$

Then,  $\int_0^T f(t) dt$  is approached by  $\sum_i^{\text{Nt}} f(\tau_i)(t_i + 1 - t_i)$ .

In a logical manner, the differential system (36) becomes

$$g(t_1) = 0, \quad (45)$$

$$\mathbf{G} \frac{g(t_{i+1}) - g(t_i)}{(t_{i+1} - t_i)} + \mathbf{M}_{zi} g(\tau_i) = \mathbf{Q}_{zi} \quad \forall i \geq 1. \quad (46)$$

Therefore, the quantity  $s_{n+1/2}$  must be defined at the integration times.

The numerical solution of the global stage is noted:  $s_{h,n+1}$ , which is not in  $A_d$ , because finite element stresses do not satisfy equilibrium equations. In order to estimate the global error, we have to build  $s_{n+1} \in A_d$  on the base of  $s_{h,n+1}$  (Fig. 11). This construction is realised through techniques, which have been developed in Cačan for 15 years [24] (Table 1).

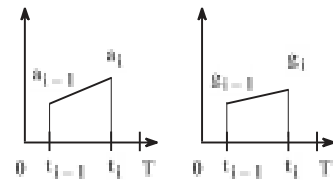


Fig. 10. Time representation.

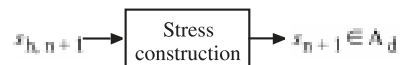


Fig. 11. Construction of admissible stress.

Table 1  
Material characteristics

$E$	200,000 MPa	$a$	300	$\lambda$	80 MPa	$R_S$	53 MPa	$m$	2
$\nu$	0.3	$c$	248,000 MPa	$Q$	80 MPa	$k$	$1/150^2$ MPa <sup>-2</sup> s <sup>-1</sup>	$R_0$	150 MPa

### 4.3. An example of few LATIN iterations

To show how the space function base works, we can give a first numerical example: a perforated plate, which is subject in its upper part to a loading described in Fig. 12. The mesh has six-node triangular elements and the time interval is divided into six-time steps. The plastic zones are represented in dark. Four iterations are performed to ameliorate the elastic initialisation. A space function for the quantities  $\underline{U}_n$ ,  $\sigma_n$ ,  $\beta_n$  and  $R_n$  has been generated at each iteration.

Let us study  $R_4$ , the isotropic hardening at the end of the fourth iteration. Four space functions constitute the base. They are represented on the left of Fig. 13 and they are classified in order of appearing downwards. The components on this base of the approximation of the isotropic hardening are represented on the right on the same figure. These components are time functions computed at the fourth global stage. Moreover, we reported the operation + and  $\times$  to schematise the sum of the products of a space function by a time function. Similar figures should have been done for the quantities  $\underline{U}_4$ ,  $\sigma_4$  and  $\beta_4$ . We can also observe the improvement of the relationship between the admissible quantities  $\sigma_{4,y,y}$  and  $\varepsilon_{4,y,y}$  (e.g.) at the maximum loading point A (Fig. 14).

In conclusion, while the number of iteration increases, non-linearities seems to be better taken into account on the interval  $[0, T]$  (Fig. 14) and the base of space functions is improved (Fig. 13). Then, if the mesh and the time discretisation are sufficiently fine, the proposed LATIN algorithm can provide a good approximation of the exact solution of the reference problem.

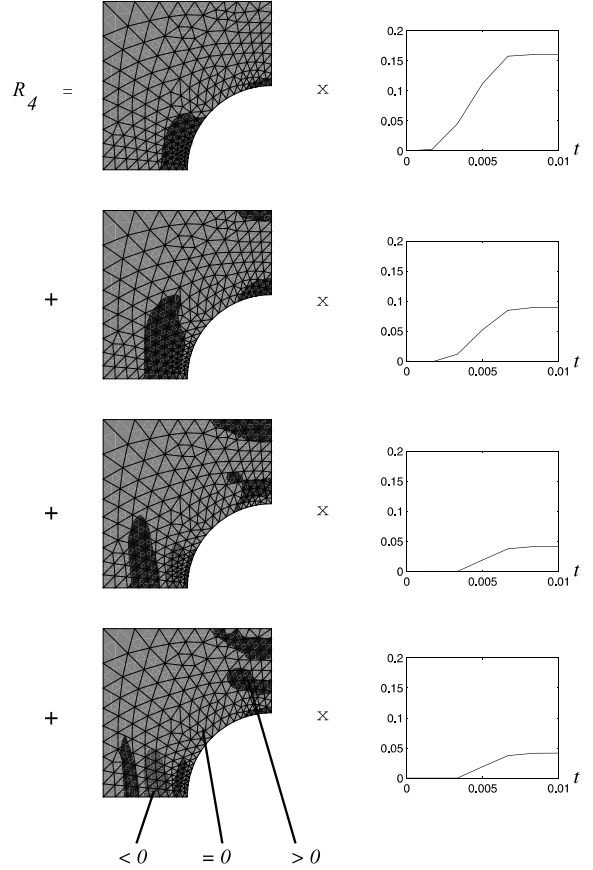


Fig. 13. An approximation of the isotropic hardening  $R_4$ .

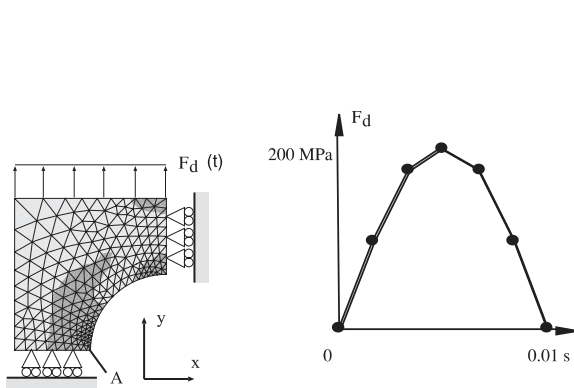


Fig. 12. Plastic zones, loading and discretisation.

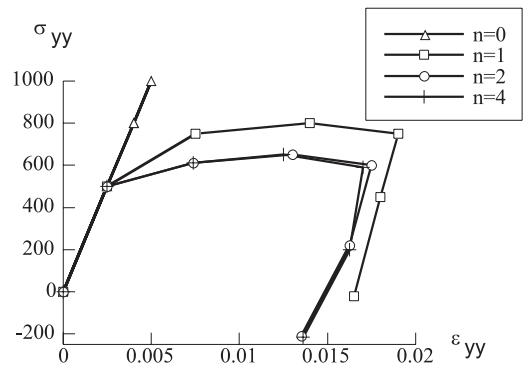


Fig. 14. Example of the improvement of the non-linear relationship between admissible stress and strain.

## 5. Error indicators for adaptation

One of the main advantages of the LATIN is to enable to control the errors after each iteration (Fig. 15). This is due to the computation on  $\Omega \times [0, T]$  of the admissible solution.

In order to simplify the notations, we are going to use  $s$  and  $s_h$  instead of  $s_{n+1}$  and  $s_{h,n+1}$ , respectively. There are numerous error sources, which all contribute to the global error estimator  $e_{\text{ref}}$ . The difficulty is to separate these contributions through error indicators. These indicators must be efficient enough to enable to pilot the resolution algorithm in the various cases. The parameters to adapt are the mesh, time discretisation and the number of iterations. We therefore need three error indicators at least. Our approach to define these indicators consists in exploiting the notion of reference associated to the error control. We demonstrate that these indicators provide a partition of the global error. A definition of plasticity visibility is also presented in this section.

### 5.1. A geometric approach

Before developing the equations, we are going to present the main points of the approach, which are used to define the indicators. During the conception of the numerical resolution algorithm, we introduced in order approximations, which are specific to the LATIN method  $L_{\text{ap}}$ , approximations associated to the finite element method  $h_{\text{ap}}$ , and approximations associated to the time integration scheme  $\Delta t_{\text{ap}}$ . This can be schematised in Fig. 16, in which  $P_{\text{num}}$  is the numerical global stage of the last LATIN iteration.

We can also consider the classification of the approximations, appearing in Fig. 17.

Between  $P_{\text{ref}}$  and  $P_{\text{num}}$ , we can define intermediate problems (Fig. 18):

- a non-linear finite element problem, which is continuous in time  $P_h$ ,

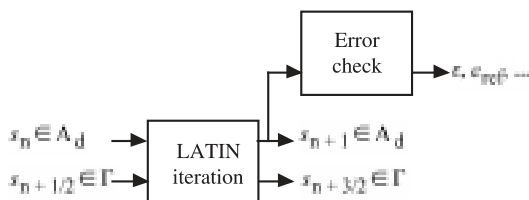


Fig. 15. Error control during the computation.

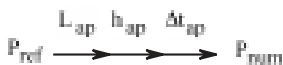


Fig. 16. Amount of approximations.



Fig. 17. Classification of the approximations, in order to define the error indicators.



Fig. 18. Intermediate problems.

- a non-linear finite element problem with a numerical time integration scheme  $P_t$ .

As for the reference problem, we are going to define the admissibility sets  $A_{dh}$  and  $A_{dt}$  such that

- the exact solution of  $P_h$  is defined by  $A_{dh} \cap \Gamma$ ,
- the exact solution of  $P_t$  is defined by  $A_{dt} \cap \Gamma$ .

Two additional dissipation errors can be defined. The first one is associated to the reference problem  $P_h$ :  $I_{\text{time}} = e(s_t)$  with  $s_h \in A_{dh}$ .  $I_{\text{time}}$  characterises both the approximations  $\Delta t_{\text{ap}}$  and  $L_{\text{ap}}$ . It is usually called time error indicator. The second additional dissipation error is associated to the reference problem  $P_t$ :  $I_{\text{NL}} = e(s_t)$  with  $s_t \in A_{dt}$ .  $I_{\text{NL}}$  is an indicator, which characterises the convergence defaults of the numerical global stage. These properties are represented in Fig. 19.

By comparing  $e_{\text{ref}}$  and  $I_{\text{time}}$ , we are able to obtain a space error indicator  $I_h$ . A comparison between  $I_{\text{time}}$  and  $I_{\text{NL}}$  provides a time discretisation error indicator  $I_{\Delta t}$ . The relative indicators are defined as follows:

$$\varepsilon_h = \frac{I_h}{D}, \quad \varepsilon_{\text{time}} = \frac{I_{\text{time}}}{D}, \quad \varepsilon_{\Delta t} = \frac{I_{\Delta t}}{D}, \quad \varepsilon_{\text{NL}} = \frac{I_{\text{NL}}}{D}, \quad (47)$$

where  $D$  is defined in Eq. (18).

All the equations are not developed here and only the definition of the space indicator is presented. For more details the reader can consult Ref. [23].

### 5.2. The space error indicator

The main difficulty is to define  $P_h$  in order to compare  $e_{\text{ref}}$  and  $I_{\text{time}}$ . To do so, we choose to keep the same evolution laws for  $P_h$  and  $P_{\text{ref}}$ . These equations are

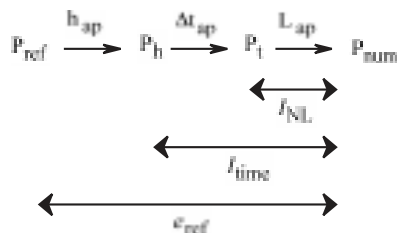


Fig. 19. Different dissipation errors.

characterised by  $\Gamma$ . Then, we can use the function  $e$  to define  $I_{\text{time}}$  and  $e_{\text{ref}}$ . All the space approximations are reported in the definition of  $A_{dh}$ .

$A_{dh}$  is defined by

- initial conditions (5),
- finite element representation and the kinematic equation,  $\underline{U} \in \mathcal{U}_h^{[0,T]}$

$$\underline{U}(\underline{M}, t) = \mathbf{N}(\underline{M})q(t) \quad \forall (\underline{M}, t) \in \Omega \times [0, T], \quad (48)$$

$$\underline{U}|_{\partial_t \Omega} = \underline{U}_d \quad \forall t \in [0, T], \quad (49)$$

- finite element equilibrium,  $\boldsymbol{\sigma} \in \mathcal{S}_h^{[0,T]}$
- $$\forall t \in [0, T] \quad \forall \underline{U}^* \in \mathcal{U}_{ho}, \quad (50)$$

$$\sum_{i=1}^{\text{Nh}} \text{Tr}[\boldsymbol{\sigma} \boldsymbol{\varepsilon}(\underline{U}^*)]_{|\underline{M}_i} w_i = \int_{\Omega} \underline{f}_d \cdot \underline{U}^* d\Omega + \int_{\partial_2 \Omega} \underline{F}_d \cdot \underline{U}^* dS,$$

- state equations at the integration points

$$\forall i \in \{1, \dots, \text{Nh}\} \quad \forall t \in [0, T] \begin{cases} \boldsymbol{\varepsilon}_{|\underline{M}_i}^p = (\boldsymbol{\varepsilon}(\underline{U}) - \mathbf{K}^{-1} \boldsymbol{\sigma})_{|\underline{M}_i}, \\ \mathbf{X}_{|\underline{M}_i} = \mathbf{A}^{-1} \mathbf{Y}_{|\underline{M}_i}, \end{cases} \quad (51)$$

- Special space representation

$$\forall i \in \{1, \dots, \text{Nh}\} \quad \forall (\underline{M}, t) \in \Omega_i \times [0, T], \quad (52)$$

$$s(\underline{M}, t) = s(\underline{M}_i, t),$$

where the domain,  $\Omega_i$  is associated to the integration point  $\underline{M}_i$  such that:  $\underline{M}_i \in \Omega_i$  and  $\text{mes}(\Omega_i) = w_i$ . The shape of  $\Omega_i$  has no importance. An example is given in Fig. 20 for a six-node triangular element with three integration points.

A special representation is introduced in order to obtain a unique solution  $s_h$  defined on  $\Omega \times [0, T]$ , which is built on the basis of the numerical results of the global stage. To obtain  $s_h \in A_{dh}$ , we just have to extend the value obtained at each integration point  $\underline{M}_i$  to the domain  $\Omega_i$ .

Thanks to the representation, the quantities  $\dot{\mathbf{X}}_h$  and  $\mathbf{Y}_h$  satisfy the admissibility conditions associated to  $P_{\text{ref}}$ . The difference between  $s \in A_d$  and  $s_h \in A_{dh}$  is due to:

- the reconstruction of a stress, which rigorously satisfies the equilibrium equation,

- the strain space representation, which is not classical because we only take into account the value of strain in the integration points to build  $s_h$ .

$$s - s_h = (\Delta \dot{\boldsymbol{\varepsilon}} - \mathbf{K}^{-1} \Delta \dot{\boldsymbol{\sigma}}, 0, \Delta \boldsymbol{\sigma}, 0) \quad (53)$$

$$\text{with } \Delta \boldsymbol{\sigma} = \boldsymbol{\sigma} - \boldsymbol{\sigma}_h \quad \boldsymbol{\sigma} \in \mathcal{S}_{\text{ad}}^{[0,T]}, \quad \boldsymbol{\sigma}_h \in \mathcal{S}_h^{[0,T]}, \quad \forall i \in \{1, \dots, \text{Nh}\} \quad \forall (\underline{M}, t) \in \Omega_i \times [0, T] \quad \Delta \boldsymbol{\varepsilon} = \boldsymbol{\varepsilon}(\underline{U}) - \boldsymbol{\varepsilon}(\underline{U})_{|\underline{M}_i}.$$

When studying the difference  $e_{\text{ref}} - I_{\text{time}}$ , we obtain the following partition of the global error:

$$e_{\text{ref}} = I_{\text{time}} + I_h + C \quad (54)$$

with

$$\dot{x} = (\dot{\boldsymbol{\varepsilon}}^p, \dot{\mathbf{X}}_h), \quad y = (\boldsymbol{\sigma}, \mathbf{Y}_h), \quad \dot{x}_h = (\dot{\boldsymbol{\varepsilon}}_h^p, \dot{\mathbf{X}}_h),$$

$$y_h = (\boldsymbol{\sigma}_h, \mathbf{Y}_h), \quad I_h = \int_{\Omega} i_h d\Omega,$$

$$i_h = \int_0^T \{ \varphi(\dot{x}) - \varphi(\dot{x}_h) - \partial_x \varphi(\dot{x}_h) \cdot (\dot{x} - \dot{x}_h) \} dt \\ + \int_0^T \{ \varphi^*(y) - \varphi^*(y_h) - \partial_y \varphi^*(y_h) \cdot (y - y_h) \} dt \\ + \frac{1}{2} \text{Tr}[\mathbf{K}^{-1}(\boldsymbol{\sigma} - \boldsymbol{\sigma}_h)(\boldsymbol{\sigma} - \boldsymbol{\sigma}_h)]_{|t=T},$$

$$C = \int_0^T \int_{\Omega} \text{Tr}[\Delta \boldsymbol{\sigma}(\partial_{\boldsymbol{\sigma}} \varphi^*(y_h) - \dot{\boldsymbol{\varepsilon}}_h^p)] d\Omega dt \\ + \int_0^T \int_{\Omega} \text{Tr}[\mathbf{K}^{-1} \Delta \dot{\boldsymbol{\sigma}}(\partial_{\dot{\boldsymbol{\varepsilon}}} \cdot p\varphi(\dot{x}_h) - \boldsymbol{\sigma}_h)] d\Omega dt \\ + \int_0^T \int_{\Omega} \text{Tr}[\Delta \dot{\boldsymbol{\varepsilon}}(\partial_{\dot{\boldsymbol{\varepsilon}}} \cdot p\varphi(\dot{x}_h) - \boldsymbol{\sigma}_h)] d\Omega dt.$$

A part of  $I_h$  corresponds to the elastic error in constitutive relation [24]:

$$\frac{1}{2} \int_{\Omega} \text{Tr}[\mathbf{K}^{-1}(\boldsymbol{\sigma} - \boldsymbol{\sigma}_h)(\boldsymbol{\sigma} - \boldsymbol{\sigma}_h)]_{|t=T} d\Omega.$$

In fact,  $I_h$  is similar to a sum of distances between  $s \in A_d$  and  $s_h \in A_{dh}$ . This is why we are going to use  $I_h$  as a space error indicator. Local information for the mesh adaptation is obtained through  $i_h$ . The quantity  $C$  is the sum of coupling terms between different defaults. A similar partition of  $I_{\text{time}}$  can be obtained.

### 5.3. Elasticity and plasticity visibility

When a mesh is coarse, it may not enable to consider plasticity. In such case, there is a problem of plasticity visibility.

**Definition 1.** Consider the computation of an admissible solution  $s_h$  with an elastic approximation of the material behaviour:  $s_h \in A_{dh} \cap \Gamma_e$ . The plasticity is visible through the mesh if and only if the error sources are not limited to the space errors. This can be written as follows:

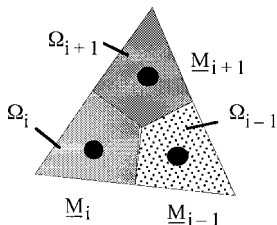


Fig. 20. Domains used to build  $s_h \in A_{dh}$ .

$$\varepsilon_{\text{time}} \neq 0, \quad (55)$$

which amounts to saying that there is at least one integration point in the plastic zone. If the plasticity is not visible through the mesh, it is then needless to consider performing a non-linear computation. With  $\varepsilon_{\text{time}}$  and the prescribed global quality  $\varepsilon_0$ , it is also possible to observe if the plasticity is significant.

**Definition 2.** The plasticity is significant if and only if

$$\varepsilon_{\text{time}} > \frac{\varepsilon_0}{\lambda} \quad \text{with } \lambda > 1. \quad (56)$$

(In practice we use  $\lambda = 0.5$ .) If the plasticity is not significant, the mesh can be adapted as if the problem were elastic to obtain the prescribed quality  $\varepsilon_0$ .

## 6. The non-incremental adaptive strategy

In this section, we present the adaptive strategy based on the non-incremental algorithm and the error indicators introduced above. The main idea is to utilise the solution improvement process, which is obtained through the LATIN method. In the course of the iterations, the admissible solution satisfies the non-linear equations to a greater extent. However, in the beginning, the computation is very far from the solution. We therefore do not need to use fine discretisation to represent the first coarse corrections. In order to reduce the cost of the simulation, we suggest to adapt the discretisation in the course of the iterations of the LATIN method in order to obtain balanced contributions to the global error.

### 6.1. The framework of the strategy

The error control during the computation enables to master:

- the number of iteration through the global relative error  $\varepsilon_{\text{ref}}$ ,
- the mesh through the space error indicator  $I_h$ ,
- and the time discretisation through  $I_{\Delta t}$ .

Classical mesh adaptation or time discretisation adaptation are possible after each error checking. In order to continue the computation, the admissible solution has to be transferred on the new discretisation (Fig. 21).

In case of mesh adaptation, the admissible solution  $s_h$  before adaptation becomes  $\tilde{s}_h$  after the projection. This projection is done when the space functions are represented with the new mesh. We first transfer to new integration points, the values of

$$(\underline{\mathbf{e}}(\underline{\mathbf{A}}_k))_{k=1\dots N_u}, \quad (\mathbf{B}_k)_{k=1\dots N_s} \quad \text{and} \quad (\mathbf{C}_k)_{k=1\dots N_y}$$

to obtain

$$(\hat{\underline{\mathbf{e}}})_{k=1\dots N_u}, \quad (\hat{\mathbf{B}}_k)_{k=1\dots N_s} \quad \text{and} \quad (\hat{\mathbf{C}}_k)_{k=1\dots N_y}$$

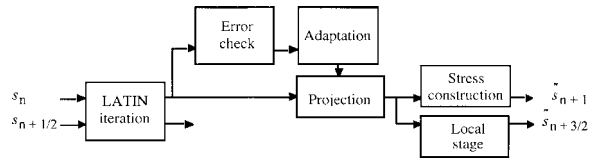


Fig. 21. Adaptive iteration.

Then,  $(\hat{\underline{\mathbf{e}}})_{k=1\dots N_u}$  and  $(\hat{\mathbf{B}}_k)_{k=1\dots N_s}$  are modified into admissible fields through a minimisation associated to an elastic energy. Before following the iteration, a local stage provides  $\tilde{s}_{n+3/2}$ .

### 6.2. Piloting criteria

The piloting criteria of adaptation are very simple. Error contributions are said to be balanced if and only if space defaults are close to the rest of the defaults:

$$0.1\varepsilon_{\text{time}} < \varepsilon_h < \varepsilon_{\text{time}}, \quad (57)$$

time discretisation defaults are close to the numerical convergence defaults:

$$0.01\varepsilon_{\text{NL}} < \varepsilon_{\Delta t} < 0.5\varepsilon_{\text{NL}}. \quad (58)$$

If  $\varepsilon_h \geq \varepsilon_{\text{time}}$ , then the mesh is too coarse to continue the LATIN corrections without a mesh adaptation. If  $\varepsilon_h \leq 0.1\varepsilon_{\text{time}}$ , then the mesh is too fine, and the LATIN iteration is too expensive.

We add to these criteria the following rules:

- *R1*: after the initialisation, if plasticity is significant, then a first iteration is made with the coarse mesh. If this is not the case, the mesh is automatically refined to get a better elastic initialisation.
- *R2*: after each mesh adaptation, one iteration at least is made, even if error contributions are not balanced. Some rules are added to limit the number of error controls. The global error and the space error indicator are not computed at each iteration.

### 6.3. A detailed example

We consider the adaptive computation of the perforated plate presented in Section 2. The aim is to obtain a global dissipation error estimate equal to 5% ( $\varepsilon_0 = 5\%$ ). The initial mesh is M1 (Fig. 22) and the interval  $[0, T]$  is divided into six subintervals.

The evolution of the global error,  $\varepsilon_h$  and  $\varepsilon_{\text{time}}$  during the iteration, are presented Fig. 23. In the course of the computation, the mesh is adapted three times. The adapted meshes are M2, M3 and M4 (Fig. 24). The analysis is conducted with six-node triangular elements.

An elastic computation with M1 (40 elements) allows us to initialise the resolution with an admissible solution  $s_0$ . Using this approximation, the global error computed is  $\varepsilon_{\text{ref}} = 36\%$ , the space error indicator is  $\varepsilon_h = 29\%$ , and

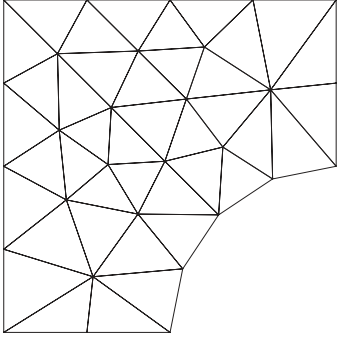


Fig. 22. Initial mesh M1.

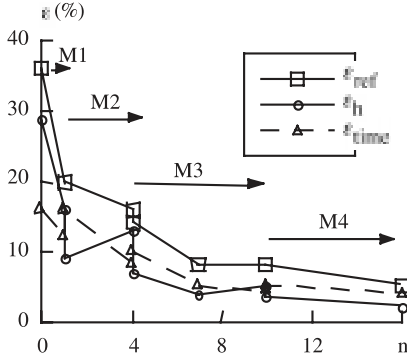
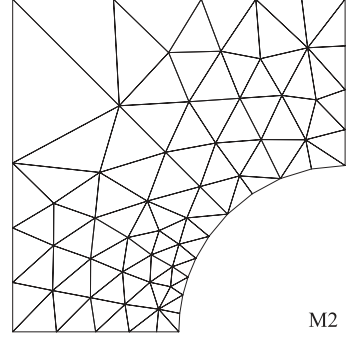


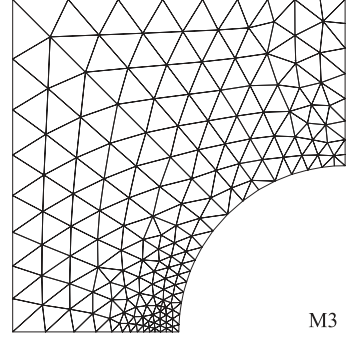
Fig. 23. Error controls during the iterations.

$\varepsilon_{time} = 16\%$ . Plasticity is significant ( $\varepsilon_{time} > 0.5\varepsilon_0$ ). Then, an initial iteration is performed to take better account of plasticity in the admissible solution (Rule R1). Thus, the error computation gives:  $\varepsilon_{ref} = 20\%$ ,  $\varepsilon_h = 16\%$ ,  $\varepsilon_{time} = 12\%$ . At the end of this first iteration, space error are too high in comparison with the other error sources ( $\varepsilon_h > \varepsilon_{time}$ ). Thanks to the local contribution  $i_h$ , a new mesh M2 (94 elements) is automatically built to reduce the space error. Data are transferred from the mesh M1 to the mesh M2, and an error control is realised:  $\varepsilon_{ref} = 20\%$ ,  $\varepsilon_h = 9\%$ ,  $\varepsilon_{time} = 16\%$ . We notice that space errors have obviously decreased, and the error sharing has been modified ( $\varepsilon_{time} \approx 1.8\varepsilon_h$  instead of  $\varepsilon_{time} \approx 0.6\varepsilon_h$ ). The following iterations improve the integration of the non-linear finite element problem:  $\varepsilon_{time}$  decreases. Three iterations are done before a new mesh adaptation. The new adapted mesh is M3 (333 elements). The different error levels are balanced ( $\varepsilon_{ref} = 14\%$ ,  $\varepsilon_h = 7\%$ ,  $\varepsilon_{time} = 10\%$ ). At the end of the 10th iteration, the mesh has to be changed ( $\varepsilon_h > \varepsilon_{time}$ ). The mesh M4 is built (1362 elements). At the end of the 16th iteration, the global error represents 4.9%. The aim has been reached.

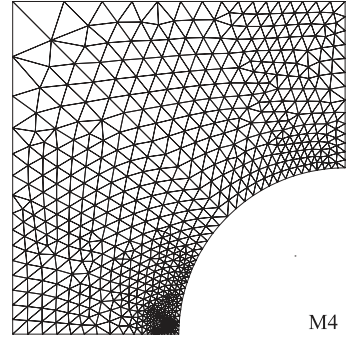
During this computation, the time discretisation has been adapted at the end of 12th iteration. The third and fourth time subintervals have been cut into two equal parts.



M2



M3



M4

Fig. 24. Adapted meshes.

#### 6.4. An example where plasticity is negligible

In the previous example, by reducing the loading intensity, the size of the plastic zones decreases. Let us study a maximum loading equal to 80 MPa.

We still start the adaptive computation with the same mesh M1 (Fig. 22). After the elastic initialisation, the error computation gives:  $\varepsilon_{ref} = 18\%$ ,  $\varepsilon_h = 18.5\%$ ,  $\varepsilon_{time} = 0.5\%$ . Plasticity is not significant ( $\varepsilon_{time} < 0.5\varepsilon_0$ ). Then, the mesh is adapted to improve the elastic computation. The new mesh is M2 (Fig. 25) and we obtain:  $\varepsilon_{ref} = 5\%$ ,  $\varepsilon_h = 4\%$ ,  $\varepsilon_{time} = 0.8\%$ . The aim is reached without any plastic computation although plasticity exists ( $\varepsilon_{time} > 0$ ). In this case, plastic strains can be estimated with local computations.

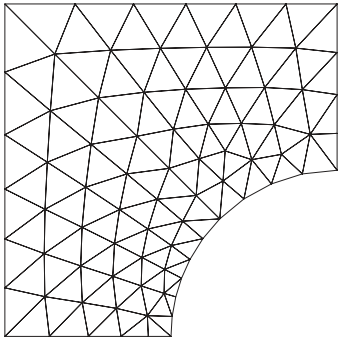


Fig. 25. Mesh adapted through an elastic computation.

### 6.5. Efficiency of the strategy

Thanks to the use of coarse discretisation to start the simulation, the time needed to prepare the computation is reduced, because coarse mesh are very easy to obtain. Moreover, by balancing the error contributions during the iterations, this strategy allows to reduce the computation itself, for a given quality. To quantify this cost reduction, we compare the CPU time of our adaptive computation to the CPU time of a reference computation. This reference computation is similar to an expert's computation, where the adapted discretisation is known in order to obtain the prescribed quality. Here, this adapted discretisation is provided through the adaptive strategy. Moreover, the reference computation is made through the LATIN algorithm with the same discretisation during all the iteration.

### 6.6. Example of efficiency

To illustrate the reduction of the cost computation, we present the adaptive computation of a complex problem. Loading and plastic zones are presented in Fig. 26.

The evolution of the global error and  $\varepsilon_h$  during the iteration are presented in Fig. 27. The mesh has been

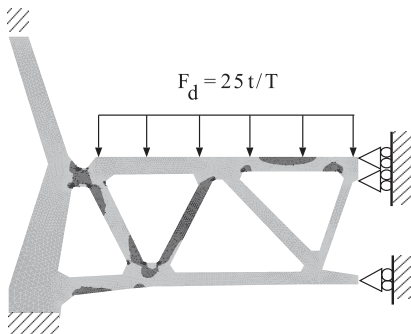


Fig. 26. Loading and plastic zones.

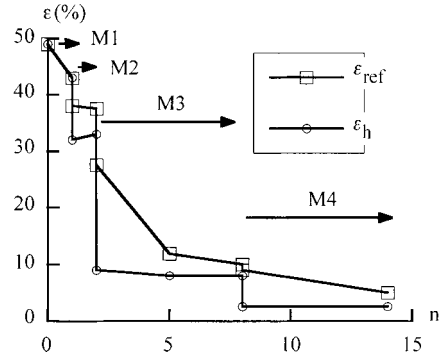


Fig. 27. Error checks during the iterations.

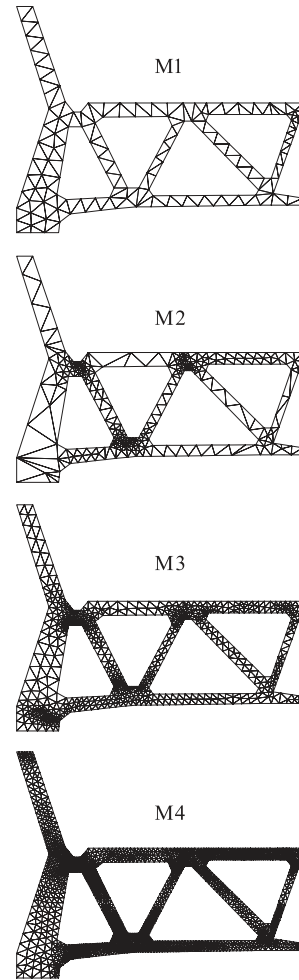


Fig. 28. Adapted meshes.

adapted three times. These adaptations appear at the end of the first, second and eighth iterations. The meshes are presented in Fig. 28. The aim has been reached in 14 iterations ( $\varepsilon_{ref} = 5.1$ ).

The reference computation is completely made with the mesh M4. The aim is reached in 13 iterations. The CPU time (on hp700 computer) needed for this computation is twice as high as that of the adaptive strategy. Thus, our adaptive strategy allows to reduce the computation cost for a given quality.

## 7. Conclusion

The LATIN method is well suited for adaptive computations based on error control, because it allows an effective improvement in the numerical solution over the entire time interval.

By balancing the error contributions during the computation, we obtain lower computation cost. We can say that the proposed strategy allows to adapt the computational effort during the iteration in comparison with the convergence defaults.

Thanks to the partition of the global error into error indicator for each kind of approximation, the piloting criteria are simple and robust, whatever the level of plasticity is.

## References

- [1] Ladevèze P. Comparaison de modèles de milieux continus. Thèse d'état, Université Pierre et Marie Curie, 1975.
- [2] Babuska I, Rheinboldt WC. A posteriori error estimates for adaptive finite element computation. *Int J Numer Meth Engng* 1978;12:1597–615.
- [3] Zienkiewicz OC, Zhu JZ. A simple error estimator and adaptive procedure for practical engineering analysis. *Int J Num Meth Engng* 1987;24:337–57.
- [4] Babuska I, Rheinboldt WC. Computational error estimates and adaptive processes for some nonlinear structural problems. *Comput Meth Appl Mech Engng* 1982;34:895–937.
- [5] Coffignal G. Optimisation et fiabilité des calculs par éléments finis en élastoplasticité. Thèse d'Etat, Université Paris VI, 1987.
- [6] Johnson C, Hansbo P. Adaptive finite elements methods for small strain elasto-plasticity. IUTAM Conference on Finite Inelastic Deformations – Theory and Applications. University of Hannover, 1991. p. 19–23.
- [7] Peric D, Yu J, Owen DRJ. On error estimates and adaptivity in elasto-plastic solids: applications to the numerical simulation of strain localisation in classical and Cosserat continua. *Int J Numer Meth Engng* 1994;37:1351–79.
- [8] Ladevèze P. Sur une famille d'algorithmes en Mécanique des Structures. *Comptes Rendus de l'Académie des Sciences, Paris* 1985;300(II):41–4.
- [9] Ladevèze P. Mécanique non linéaire des Structures. Etudes en mécanique des matériaux et des structures, Hermès, 1996.
- [10] Halphen B, Nguyen QS. Sur les matériaux standards généralisés. *J Mécanique* 1975;14:38–62.
- [11] Owen DRJ, Hinton E. Finite elements in plasticity. Swansea: Pineridge; 1980.
- [12] Bass JM, Oden JT. Adaptive finite element methods for a class of evolution problems in viscoplasticity. *Int J Engng Sci* 1987;25(6):623–53.
- [13] Belytschko T, Yeh IS. Adaptivity in nonlinear structural dynamics with contact-impact. Adaptive, Multilevel Hierarch Computat Strateg AMD, ASME 1992;157:165–202.
- [14] Zeng LF, Wiberg NE. Spatial mesh adaptation in semi-discrete finite element analysis of linear elastodynamic problems. *Computat Mech* 1992;9:315–32.
- [15] Barthold FJ, Schmidt M, Stein E. Error estimation mesh adaptivity for elasto-plastic deformations. In: Owen DRJ, Oñate E, Hinton E, editors. *Comp Plas Fund Appl, CIMNE, Barcelona*, 1997. p. 597–602.
- [16] Chaboche JL. EVP CYCL: Un code d'éléments finis en viscoplasticité cyclique. La recherche aérospaciale 1986. p. 91–112.
- [17] Choi CK, Chung J. An adaptive control of spatial-temporal discretization error in finite element analysis of dynamic problems. *Struc Engng Mech* 1995;3(4):391–410.
- [18] Tie B, Aubry D. Error estimates, h adaptative strategy and hierarchical concept for non-linear finite element method. *Numer Meth Engng*, 1992.
- [19] Gallimard L, Ladevèze P, Pelle JP. Error estimation and adaptivity in elastoplasticity. *Int J Numer Meth Engng* 1996;39:189–217.
- [20] Moës N. Une méthode de mesure d'erreur a posteriori pour les modèles de matériaux décrits par variables internes. Thesis, Ecole Normale Supérieure de Cachan, 1996.
- [21] Coorevits P, Ladevèze P, Pelle JP. Mesh optimization for problems with steep gradients areas. *Engng Computat* 1994;11(2):129–44.
- [22] Artz M, Cognard JY, Ladevèze P. An efficient computational method for complex loading histories. In: Owen DRJ, Oñate E, Hinton E, editors. *Comp Plas Fund Appl, Barcelona*, 1992. p. 225–36.
- [23] Ryckelynck D. Sur l'analyse des structures viscoplastiques: stratégie adaptative et contrôle de qualité. Thesis, Ecole Normale Supérieure de Cachan, 1998.
- [24] Ladevèze P, Pelle JP, Rougeot P. Error estimation and mesh optimization for classical finite elements. *Engng Computat* 1991;8:69–80.